Registration Tasks for a Hybrid Tracking System for Medical Augmented Reality

Bernd Schwald Helmut Seibert
Computer Graphics Center (ZGDV), Department Visual Computing
Fraunhoferstraße 5
D-64283 Darmstadt, Germany
{bernd.schwald,helmut.seibert}@zgdv.de

ABSTRACT

Tracking technologies for medical Virtual or Augmented Reality (VR/AR) applications have to fulfill demanding requirements. A hybrid tracking system can merge positive attributes of different tracking technologies, for example optical and electromagnetic, and try to compensate the bad ones. The alignment of two or more tracking systems by means of transforming all measured data from different systems into one common coordinate system is a fundamental precondition. Usage and processing of time stamps assigned to each measurement is a very effective element in order to achieve a higher accuracy in the alignment procedure and during later use. The algorithms for the alignment of tracking systems can also be used for the registration of the patient, another typical task in medical VR/AR applications. This paper describes both procedures in detail, including algorithms and results from test sequences. The representative tests illustrate, that the proposed algorithms provide satisfying results. An overview of the integration of the hybrid tracking system in a medical AR system is given. Adverse conditions like environmental influences on the tracking systems and the identification of corresponding measurements of two tracking systems are discussed.

Keywords

Tracking, Hybrid, Registration, Augmented Reality, Virtual Reality, Interaction

1. INTRODUCTION

Medical domains like minimal invasive surgery offer very interesting fields of application for Virtual Reality (VR) and Augmented Reality (AR). Usually there is no real view on the area of intervention because it is located inside the patient. The physician has to perform interventions on basis of his experience and preoperative image data, for example from a CT or MRI scan, that is presented without respect to the real patient or the instrument used for the intervention.
A virtual model of the area of intervention based on image data obtained in a preoperative step in combination with a tracked instrument offers the possibility to generate this respect and can support the navigation with the instrument, by showing the real interaction in the virtual world. The usage of AR technologies goes one step further and establishes the respect of the virtual model to the real patient by superimposing him.
One essential component of such an AR system is the tracking system. The accuracy of the tracking system and the registration of objects in the augmented environment is still a very challenging task. The AR system [17, 18, 22], motivating the work presented in this paper, consists besides other components in a hybrid tracking system combining video-based infrared marker tracking with an electromagnetic tracking system. The reasons for the choice of a hybrid approach are described and a short overview of the AR system including a more detailed description of the tracking systems is given in section 2. The focus of this paper is on the alignment and registration tasks needed for the simultaneous utilization of two tracking systems and their performance. Section 3 describes the determination of the common coordinate system for two tracking

Journal of WSCG, Vol.12, No.1-3, ISSN 1213-6972
WSCG'2004, February 2-6, 2004, Plzen, Czech Republic.

systems. The algorithms for this process based on two different methods, are presented along with the results of several tests. Problems caused by a time offset between the systems and different respectively changing update rates are discussed.
Section 4 describes how the virtual model of the patient is registered to the real patient. Analogous to section 3, methods and results from various tests are presented.
Conclusion and future work of this ongoing research and development can be found in section 5.

2. AR ASPECTS AND TRACKING SYSTEMS

The background for the work presented in this paper is a prototypical medical AR system [17, 18], which is developed in an ongoing research project [22]. One special attribute of this system is a transparent display, providing the user (physician) with an augmented view of the patient avoiding the need to wear a Head Mounted Display as shown in [2]. This transparent display is mounted on a swivel arm and can be moved easily over the area of interest, i.e. the patient, see figure 1. The user gets the virtual 3d model of the patient's anatomy, especially the region of intervention, and the virtual model of his instrument, which is partially inserted into the patient's body, as additional information projected into his view.

Figure 1. Augmented Reality System for minimal invasive surgery. Infrared cameras track the AR display. Eyeglasses and instrument are lying on the table.

Some requirements for the tracking system can be defined outgoing from this setup. The poses of the user, the transparent display and the patient have to be known, to allow augmentations in the user's field of view. Additionally the instrument for the intervention needs to be tracked to allow navigation support. High accuracy, best below 1*mm* positional accuracy and an appropriate accuracy of orientation is a requirement for all objects to track. Furthermore the tracking of the head of the user should be wireless, in order not to restrict the freedom of movement. For the instrument, wireless tracking technology would be preferable as well. Usually the instrument is used below the transparent display, inhibiting the usage of video based tracking due to occlusion problems.
Based on these facts, a hybrid tracking system has been developed, which is combining optical tracking for user's head and the display and an electromagnetic tracking system for the registration of the patient and the tracking of the instrument. The data flow and the system architecture is comparable to the OpenTracker system [15]: arbitrary tracking devices can be connected to the system via a network communication layer.
One main task for the usage of a combined tracking system is the alignment of the two different reference coordinate systems described in section 3. Besides the accuracy, easy and fast handling of the process is important for the user.
For the AR system is not designed to be a fixed installation in one room, all components of the AR system are attached to one trolley, which can be moved easily to the desired location, for example an operation theater. The alignment process has to be repeated each time the system has been moved.
Concerning the importance of an easy and fast handling of the alignment process, the same is true for the registration of the patient; see section 4.
In the following a short overview of the two tracking systems is given.

2.1. Optical Tracking System

The optical tracking system consists in a stereo camera system. Each camera is equipped with an infrared filter and connected to a frame grabber. It is non-commercial and was developed at ZDGV. Similar tracking systems have been presented in previous work [10, 5, 16, 11, 13] and some relatively expensive commercial tracking systems are available at the market [23, 21].
The case of the transparent display is mounted with seven infrared diodes in different positions and orientations. The user has to wear a kind of eyeglass without lenses, which is also mounted with 4 infrared diodes as active markers. The two synchronized and calibrated cameras are used to detect the diodes in the two camera images. With the known geometry of the camera setup, the 3d points are reconstructed. From the different geometrical constellations of infrared diodes on the display and on the glasses, these two objects can be identified and their poses be determined, see figure 2.
The optical tracking system has a measurement rate of around 21*Hz* and a static position accuracy of approximately 1*mm* within the interaction volume of

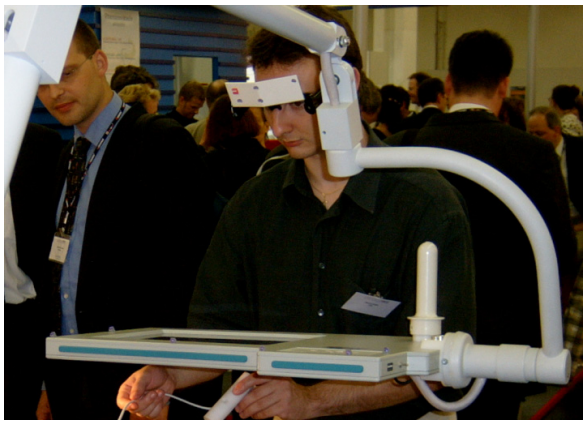

Figure 2. Glasses and transparent display, both equipped with infrared markers.

the setup, covering the needed interaction volume of around $1.5m \times 0.8m \times 1m$ (width, depth, height). Several six degrees of freedom sensors in form of rigid bodies based on geometric models of infrared markers can be tracked, only two are needed here. Each measurement is provided with a time stamp, which is created when the external trigger signal for the cameras is generated.
According to the camera and frame grabber manufacturer's documentation, a fixed delay of a few milliseconds to the start of the grabbing process needs to be expected. Environmental infrared light from luminous sources like the sun or light bulbs or even reflected light from any source can increase the measurement time or interrupt the measurement procedure. On the other hand, occlusion may interrupt the measurement at any time.

2.2. Electromagnetic Tracking System

In the current setup, the accuracy of the optical tracking is of subordinate importance for the navigation with the instrument. The important part for the navigation is the electromagnetic tracking, for which technical details from specifications of the pciBIRD can be found in table 1.

Degrees Of Freedom	6 (Position and Orientation)
Translation range	$\pm$ 76.2 cm in any direction
Static Accuracy Position	1.4mm RMS
Static Accuracy Orientation	0.5 ° RMS
Update rate	Up to 105 measurements/sec

Table 1. Some details from the technical specification of the pciBIRD from Ascension with 8mm Sensors.

The pciBIRD is used with two $8mm$ sensors allowing an easy integration into a plastic handle for an instrument or the alignment device, see figure 3. The tracking results are provided with a time stamp for each measurement. The electromagnetic tracking system gets more disturbed if the distance between emitter and sensor increases or if the sensor is moved rapidly. The appearance of these distortions cause the processing unit of the tracking system to apply some more filtering on the measured signals, which can be noticed as an increasing delay.

3. ALIGNMENT OF TRACKING SYSTEMS

The alignment procedure between the two tracking systems has to provide two results: A transformation from one reference coordinate system to the other, such that tracking results can be represented in the same coordinate system, and a time offset between the two systems. Other approaches in the area of hybrid tracking [4] discuss correction of the measurements through a look-up table with pre-calibrated correction factors. An overview about calibration and correction issues for electromagnetic tracking systems is given in [9]. The correction of the distortions, which appear in electromagnetic tracking, has not been used in our approach yet. By now the focus has been on the registration algorithm.

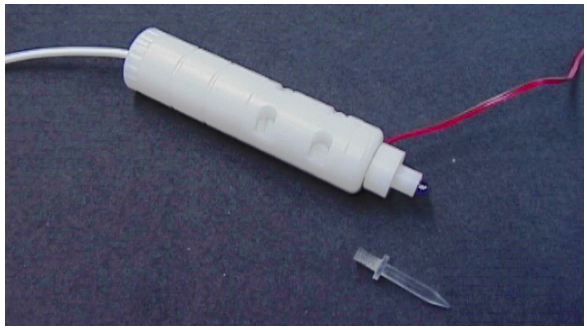

Figure 3. The alignment device with integrated electromagnetic sensor and additional infrared diode on tip.

For the user the alignment simply consists in the following procedure: He has to sway around an alignment device, consisting of a plastic handle and an infrared diode, see figure 3. This has to be done for about 20 seconds, until enough measurements, for example at least $m = 250$, from each system were recorded. The user has to take care that the alignment device does not leave the interaction range of both tracking systems. Moving close to the limit of interaction range of the electromagnetic tracking system is quite critical because the quality of measurements decreases too much. To prevent the user from doing so, a warning audio signal is emitted if a sensor is too far away from the electromagnetic emitter. After recording measurements, a few more seconds are needed for the optimization until the whole procedure is finished.

3.1. Alignment Algorithms

A certain number $n \leq m$ of corresponding 3d points (P_i, Q_i), with $1 \leq i \leq n, P_i \in \mathbb{R}^3$ from the electromagnetic tracking and $Q_i \in \mathbb{R}^3$ from optical tracking is forming the basis for the following optimization steps with the aim to find a rotation (matrix) R and a translation T minimizing

$$err = \sum_{i=1}^{n} |\underbrace{RP_i + T - Q_i}_{residual}|^2.$$

This problem can be solved easily [8] by maximizing the trace(RK), where

$$K = \sum_{i=1}^{n} \hat{Q}_i \hat{P}_i^T.$$

The points $\hat{P}_i = P_i - \bar{P}$ are obtained by shifting P_i to the centroid $\bar{P} = 1/n \sum_{i=1}^{n} P_i$, analogous for $\hat{Q}_i$ and $\bar{Q}$. Given the Singular Value Decomposition (SVD) of $K = VDU^T$, $R = VU^T$ is the optimal rotation matrix maximizing the trace. The optimal translation is computed by $T = R\bar{P} - \bar{Q}$ [19].

These results are applied to each correspondence (P_i, Q_i) and if the distance

$$d = |RP_i + T - Q_i|$$

exceeds a certain threshold, this correspondence is ignored for one second iteration step with the same algorithm, just to omit influence of heavily distorted point correspondences. The obtained rotation R and translation T after the second step are the final result. This algorithm is a kind of Iterative Closest Point (ICP) algorithm, introduced by Besl and McKay [1] and discussed in many papers during the last years.

An alternative method applying a non-linear optimization with the Levenberg-Marquardt (LM) method [12, 14] was tested. For the results yield just a slightly different mean error *err* and because of its simplicity, the first solution is preferred.

The alternative algorithm works as follows: The first step is a linear optimization with the aim to generate sufficient good initial values for the LM optimization. From the corresponding point pairs (P_i, Q_i), the matrix $A \in \mathbb{R}^{3n \times 12}$, with

$$A^T = \begin{pmatrix} x_1^P & 0 & 0 & x_2^P & \cdots & x_n^P & 0 & 0 \\ y_1^P & 0 & 0 & y_2^P & \cdots & y_n^P & 0 & 0 \\ z_1^P & 0 & 0 & z_2^P & \cdots & z_n^P & 0 & 0 \\ 1 & 0 & 0 & 1 & \cdots & 1 & 0 & 0 \\ 0 & x_1^P & 0 & 0 & \cdots & 0 & x_n^P & 0 \\ 0 & y_1^P & 0 & 0 & \cdots & 0 & y_n^P & 0 \\ 0 & z_1^P & 0 & 0 & \cdots & 0 & z_n^P & 0 \\ 0 & 1 & 0 & 0 & \cdots & 0 & 1 & 0 \\ 0 & 0 & x_1^P & 0 & \cdots & 0 & 0 & x_n^P \\ 0 & 0 & y_1^P & 0 & \cdots & 0 & 0 & y_n^P \\ 0 & 0 & z_1^P & 0 & \cdots & 0 & 0 & z_n^P \\ 0 & 0 & 1 & 0 & \cdots & 0 & 0 & 1 \end{pmatrix},$$

and the vector $b^T = (x_1^Q, y_1^Q, z_1^Q, x_2^Q, \ldots, z_n^Q)$, $b \in \mathbb{R}^{3n}$ is generated. As described in [6], the overdetermined linear equation $Ax = b$ can be solved by means of QR decomposition. Nine components of the result x form the preliminary solution matrix R' with

$$R' = \begin{pmatrix} x_1 & x_2 & x_3 \\ x_5 & x_6 & x_7 \\ x_9 & x_{10} & x_{11} \end{pmatrix}.$$

This matrix R' is not necessarily a rotation matrix, because it is not necessarily orthonormal. Therefore the new matrix R will be forced to be orthonormal by applying the SVD to R'.

While the translation T is determined by the other three components of x_4, x_8, x_{12}. This translation T and rotation R is used as initial guess for the LM optimization with the *residual* as cost function, resulting in the final rotation R and translation T.

3.2. Measuring Time Offset

The usage of different tracking systems implies a non-negligible problem because the systems are usually neither synchronized, nor capable of producing the same measurement rate. In [3] the correspondence problem is solved by discarding measurements while the sensors are in motion. This is a suitable way, if only some points need to be measured e.g. for registration issues, but it does not satisfy the needs for interaction based AR applications. The critical issues of synchronizing sensors in VR environments have been discussed in [7]. From our experience the usage of time stamps is the most reliable way to find corresponding measurements of both systems. The data streams of several tracking systems can then be synchronized, even if the tracking systems are operated at different hosts. The operating system does not necessarily provide one single high accuracy reference timer, therefore it has to be assured that the time stamps for both systems are comparable. The measurement rate of the tracking systems is not constant and the tracking systems are usually more or less affected by changes in the environment causing a decreasing respectively increasing measurement rate.

In order to provide a reliable alignment, these adverse influences have to be taken into account. Assuming that the time stamps provided with the measurement data are correct, the time stamps are used to select corresponding pairs of measurements out of the recorded set. Due to the fact that each tracking system provides a time stamp without having one single reference timer, a fixed time offset between the time stamps of the used tracking systems is expected. Additionally there may be a fixed delay between measurement and time stamp acquisition.

After the measurement period, the two sets of 3d points $P = \{P_i \in \mathbb{R}^3 | 1 \leq i \leq n_p, i \in \mathbb{N}\}$ from electromagnetic tracking and $Q = \{Q_j \in \mathbb{R}^3 | 1 \leq j \leq n_q, j \in \mathbb{N}\}$ from

optical tracking are available, both equipped with time stamps for each measured point.
Due to the characteristics of the tracking systems, mentioned in section 2.1 and 2.2 a fix time offset between the time stamps needs to be expected. In order to find this time offset, the minimization of *err*, see section 3.1, is performed for several time offsets t_{offset} in the range of $t_{min} = -0.5$ and $t_{max} = 0.5$ seconds.
The first task is to find the set of corresponding points (P_i, Q_j) with respect to the time offset t_{offset} between their time stamps, up to a certain tolerance Δt. This is nearly impossible when $\Delta t = 0$. On the other hand, a 3d point measured by one tracking system could be assigned to two or more 3d points measured by the other tracking system, if Δt is too large. Therefore Δt must be significantly smaller than the update interval of the tracking system with the highest measurement rate.
The expected number of correspondences is determined by the measurement rates of the two tracking systems and the duration of the measurement period. Due to the problems of distortion mentioned above, the number of acceptable correspondences can decrease in comparison to n_p and n_q significantly.
For a predefined time step t_{st}, each time offset $t_{offset} \in M$ with

$$M = \{t_{min} + kt_{st} | 0 \leq k \leq \frac{t_{max} - t_{min}}{t_{st}}, t_{st} \neq 0, k \in \mathbb{N}\},$$

is used to define a set of point correspondences

$$C_{t_{offset}} = \{(P_i, Q_j) | P_i \in P, Q_j \in Q, |t(P_i) + t_{offset} - t(Q_j)| < \Delta t\}.$$

The expression $t(P_i)$ denotes a function, which yields the time stamp attached to the measurement P_i.

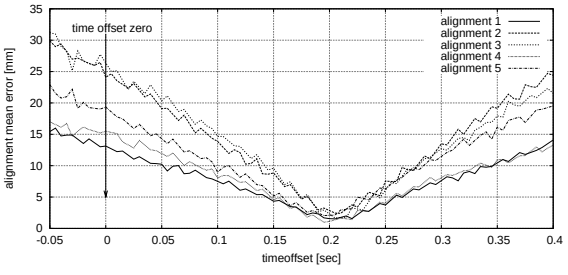

Figure 4. Resulting mean errors of the registration algorithm for a range of time offsets.

The alignment algorithm described in section 3 is applied to each set $C_{t_{offset}}$ of correspondences. The set of correspondences causing the least overall error *err*, see section 3.1, is selected and the corresponding time offset t_{offset} is assumed to be best. Figure 4 illustrates the relation between time offset and resulting mean error. The amount of $0.2sec$ time offset is bigger than expected but this result is influenced by the use of different timers in the two tracking systems.

3.3. Alignment Results

A typical setup of the tracking systems for the use in the AR environment was chosen to evaluate the algorithms. The main interaction volume is covered by the range of both tracking systems. The electromagnetic emitter is in a distance of approximately $0.3m$ from the center of the interaction volume, the cameras of the optical tracking system approximately $2m$.
Table 2 shows the results of ten tests in the same setup. The columns have the following meaning: number of the test, number of correspondences, number of ignored correspondences, the time offset between the tracking systems in milliseconds, the mean error in *mm* (see *residual* from section 3.1) after applying the calculated rotation R and translation T and the corresponding max error in *mm*.

test	corr.	ignored	time offset (msec)	mean (mm)	max (mm)
1	285	13	195	2.00	5.29
2	212	3	210	1.49	3.53
3	281	11	205	1.54	4.59
4	179	2	215	2.04	4.23
5	159	6	190	1.92	3.98
6	204	10	210	1.07	4.67
7	186	4	210	1.43	3.78
8	237	10	215	1.31	4.74
9	312	5	210	1.70	4.80
10	286	3	215	1.57	3.12
mean	234.1	6.7	207.5	1.61	4.27
stddev	53.7	4.0	8.6	0.31	0.69
max	312	13	215	2.04	5.29

Table 2. Results from ten alignments in the same setup

Table 3 shows the transformations obtained in each test, corresponding to table 2. The maximum and the standard deviation (stddev) of the translation are not given componentwise but based on the Euclidean distance between the vectors. In order to improve readability, the rotations are represented in Euler Angles (radians) instead of matrices or quaternions. Roll denotes the rotation around the x-axis, pitch around the y-axis and yaw around the z-axis.
The tests shown in tables 2 and 3 replicate the results of several laboratory tests made during the development phase. The proposed method to ignore correspondences afflicted with an above average error allows achieving good alignment results from distorted measurements.
A number of tests under the same conditions yield a small standard deviation in results. The assumption of a fixed time offset seems to be reasonable regarding the deviations of the calculated time offsets during the test series. Errors occurring by long-term drift of the timestamp sources have not been observed in our laboratory experiments yet, but the analysis and correction of such

test	Translation (mm)			Rotation (radians)		
	X	Y	Z	roll	pitch	yaw
1	635.8	113.3	217.9	0.008	-0.034	3.131
2	634.3	111.9	215.8	0.016	-0.035	3.133
3	633.8	110.4	217.1	0.009	-0.039	3.125
4	633.8	110.9	216.1	0.018	-0.038	3.132
5	633.2	110.3	218.1	0.012	-0.042	3.127
6	635.0	111.8	215.4	0.012	-0.031	3.131
7	635.7	112.6	217.1	0.011	-0.030	3.130
8	634.6	111.4	215.9	0.010	-0.034	3.128
9	634.6	112.5	215.4	0.008	-0.034	3.130
10	634.9	111.8	215.6	0.011	-0.032	3.130
mean	634.6	111.7	216.4	0.011	-0.035	3.130
stddev	1.64			0.003	0.004	0.002

Table 3. Transformations from ten alignments in the same setup.

sources-of-error are essential for further development. For the practical use of the alignment procedure, the relation between the mean error of each test in column five of table 2 and the standard deviation of the translations of all tests in table 3 is of interest. The mean of all mean errors is with $1.61mm$ of similar quality as the standard deviation of translations with $1.64mm$, which is little lower than the sum of errors of both tracking systems. This is a satisfying result within our expectations. The first value can be obtained as measure of the quality of the procedure after each alignment, but is not of further interest. The second value is a result of ten alignments in the same setup, comparing the more important result of the alignment, the translation.

4. REGISTRATION OF A PATIENT

The precondition for the use of the AR system is a successful execution of the alignment procedure for the used tracking systems. To prepare the patient registration, the patient has to be equipped with a certain number n of spherical markers, before a volume image of the patient's body and the markers is acquired by a CT- or MRI- scan. At least four, better up to ten markers are necessary. The markers itself have to remain on the patient until the AR system is used.

Those markers are identified in the volume data, see for example [20] for applicable methods, and their position $Q_i \in \mathbb{R}^3$, $1 \leq i \leq n$, is stored.

Right before the usage of the AR system, the patient is registered with a special device. This device consists in a handle with an integrated electromagnetic sensor and a short concave end fitting to the surface of the spherical markers. The concave end allows a virtual tip to point exactly to the of a spherical marker. The offset from the sensor to this virtual tip of the registration device has to be calibrated once in a previous procedure. This is performed by attaching the concave end to a spherical marker, such that the virtual tip is in the center of this marker, see figure 5, and the handle of the registration device is moved while measurements are recorded.

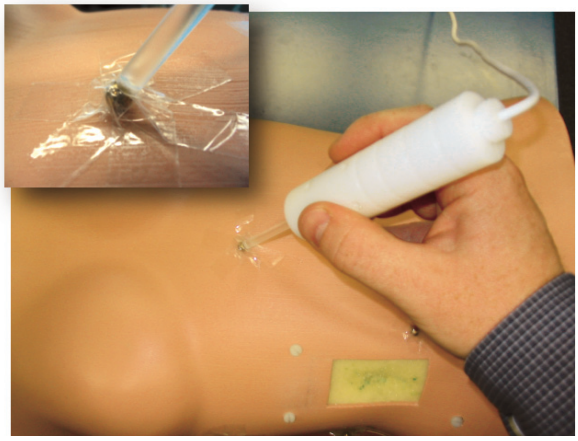

Figure 5. Registering the anthropomorphic phantom with the registration device. The concave tip is attached to a spherical marker

To get the world coordinates of the patient markers, each marker has to be registered with the registration device to acquire measurements by the electromagnetic tracking system. In order to minimize distortions several measurements, for example 100, at every position Q_i are averaged. Starting with the marker closest to the feet of a patient up to the one closest to the head, the order of the markers is well-defined.

4.1. Registration Algorithm

The patient registration is performed in a similar way as the alignment described in section 3.1. The n correspondences of 3d points (P_i, Q_i), $1 \leq i \leq n$, with $P_i \in \mathbb{R}^3$ from the electromagnetic tracking system and $Q_i \in \mathbb{R}^3$ the marker positions obtained from the volume image, are defined after the process described above. The optimization is performed in the same way, as outlined in section 3.1 with a rotation R and translation T as result. The main difference is that the set of points for the registration has less elements than the one for the alignment.

4.2. Registration Results

Analogous to the alignment tests in section 3.3, typical setups for the use in the AR environment were chosen. The registrations were performed using two different phantoms as substitute for a real patient. One phantom is a cuboid, while the other one has an anthropomorphic shape. The centroids of the markers for each phantom and each test were placed in a distance of approximately $0.3m$ from the electromagnetic emitter. The first test sequence was performed with the cuboid phantom based on eight markers, see tables 4 and 5. The markers are placed close to the corners of the cuboid. The columns have the following meaning: number of the test, the mean error in mm ($residual$) after applying the calculated rotation R and translation T, the corresponding max error in mm, the resulting

translation and rotation.

test	mean (mm)	max (mm)	Translation (mm) X	Y	Z
1	1.30	1.79	450.8	23.8	257.3
2	2.11	3.43	450.4	23.9	259.0
3	1.44	1.72	450.6	23.6	257.2
4	2.17	3.56	450.5	23.7	258.8
5	2.07	3.26	450.5	23.6	258.9
6	2.18	3.37	450.5	23.5	258.8
7	2.02	3.36	450.3	23.7	258.9
8	1.91	3.10	450.4	23.9	259.0
9	1.49	1.95	450.6	23.8	257.3
10	1.90	3.22	450.3	23.6	259.0
mean	1.86	2.88	450.49	23.71	258.42
stddev	0.327	0.741	0.826		
max	2.18	3.56	1.230		

Table 4. Results from ten registrations in the same setup with a cuboid phantom with eight markers.

test	Rotation roll	pitch	yaw
1	-1.076	-1.508	-0.517
2	-1.070	-1.506	-0.524
3	-1.045	-1.506	-0.550
4	-1.055	-1.505	-0.541
5	-1.055	-1.506	-0.541
6	-1.070	-1.508	-0.525
7	-1.078	-1.504	-0.517
8	-1.069	-1.508	-0.524
9	-1.062	-1.507	-0.532
10	-1.080	-1.507	-0.513
mean	-1.066	-1.507	-0.528
stddev	0.012	0.001	0.012

Table 5. Rotation results from ten registrations in the same setup with a cuboid phantom with eight markers.

The second test sequence, was performed with the anthropomorphic phantom, see tables 6 and 7. The nine markers are spatial not as distributed as in the first case because all are attached on the upper side of the body. In both test sequences no correspondences have been ignored because of too large deviation.

While the mean errors of the tests with the anthropomorphic phantom are smaller than those of the tests with the cuboid phantom, the standard deviations over all translations in each test series behave vice versa. The distribution of spherical markers, is for the cuboid phantom quite symmetrical, spatial well distributed and for the anthropomorphic phantom more flat, but also wider spread. A conclusion, which distribution is the better one, can not be drawn easily from our results. However, mean errors and standard deviation are at least of quite the same quality, as already observed in section 3.3.

A theoretical minimum of four markers is sufficient to perform the registration with the proposed algorithms, but the usage of a larger number of markers has to be

test	mean (mm)	max (mm)	Translation (mm) X	Y	Z
1	1.72	3.30	277.8	190.4	497.8
2	0.86	1.97	276.7	189.8	499.0
3	0.86	1.61	276.7	189.4	499.8
4	1.42	2.65	277.5	190.2	497.5
5	0.76	1.34	277.3	189.0	499.4
6	1.51	3.18	276.9	190.6	497.2
7	1.46	3.04	277.8	190.1	497.8
8	0.88	1.32	276.7	189.3	499.0
9	1.48	2.58	277.4	190.1	497.7
10	1.11	1.90	277.0	189.2	499.3
mean	1.21	2.29	277.18	189.81	498.45
stddev	0.349	0.756	1.174		
max	1.72	3.30	1.505		

Table 6. Results from ten registrations in the same setup with an anthropomorphic phantom with nine markers.

test	Rotation roll	pitch	yaw
1	0.929	1.518	-0.668
2	0.885	1.522	-0.709
3	0.894	1.522	-0.704
4	0.908	1.521	-0.687
5	0.873	1.523	-0.723
6	0.889	1.519	-0.707
7	0.935	1.520	-0.661
8	0.838	1.522	-0.757
9	0.899	1.521	-0.697
10	0.855	1.523	-0.740
mean	0.8905	1.521	-0.7055
stddev	0.0302	0.0017	0.0297

Table 7. Rotation results from ten registrations in the same setup with an anthropomorphic phantom with nine markers.

preferred due to the expected measurement errors of the tracking system. A set of eight respectively nine or ten markers seems to be a good choice in order to allow an easy and fast registration procedure with reproducible results.

Comparing the standard deviation of the rotation angles, in both test series the values for roll and yaw are quite the same, but much larger than the value for pitch. At least partially the reason for this is the representation of the rotation in Euler Angles, which do not represent rotations uniquely. If the pitch is close to $\frac{\pi}{2}$, as in the test series above, quite different values for roll and yaw can still represent the same rotation. Therefore we rank the results for the rotations of the registrations in the same way as those of the alignment in section 3.3.

Altogether the tests show that the resulting transformations are satisfying because of relatively small mean and max values on the one side and the high reproducibility on the other side.

5. CONCLUSION AND FUTURE WORK

The choice of using a hybrid tracking system is motivated by a real medical AR application. All basic requirements, resulting from this choice, i.e. the alignment and synchronization of the two tracking systems, are solved satisfying and documented in this paper in form of algorithms and test results. The accuracy of the procedures, particularly the mean translational error between 1*mm* and 2*mm* for both, the alignment and registration procedure, is within our expectations based on the accuracies of the single tracking systems.

Major improvements are still possible by using upcoming smaller sensors of electromagnetic tracking systems, which can be integrated into the tip of a registration device or a medical instrument. This could compensate the error induced by the rotation error of the sensor and the relatively large distance between sensor and tip of a device or instrument.

At the moment the two tracking systems are used hybrid in a parallel sense. Equipping an instrument with sensors of both tracking systems, at the moment this is true only for the alignment device, would allow using the hybrid system in the sense of sensor fusion. This could make the system more reliable and comfortable for real use in medical environments. Additionally the alignment procedure could be performed on-line during operation repeatedly in certain time intervals. The initial alignment procedure would become obsolete and the time to prepare the AR system could be reduced.

While the electromagnetic tracking is interesting, because of its steady data output, i.e. there are no occlusion problems, the sensor fusion would allow checking for interferences in metallic environments, thanks to the fusion with a sensor of the optical tracking system.

References

[1] P. Besl and N. McKay. A Method for Registration of 3-D Shapes. In *IEEE Trans. Pattern Anal. Machine Intell.*, volume 14, pages 239–256, 1992.

[2] W. Birkfellner, K. Huber, F. Watzinger, M. Figl, F. Wanschitz, R. Hanel, D. Rafolt, R. Ewers, and H. Bergmann. Development of the Varioscope AR: A See-through HMD for Computer-Aided Surgery. *In Proceedings International Symposium Augmented Reality - ISAR*, pages 47–53, 2000.

[3] W. Birkfellner, F. Watzinger, F. Wanschitz, et al. Calibration of Tracking Systems in a Surgical Environment. *IEEE Transactions on Medical Imaging*, 17(5):737–742, 1998.

[4] W. Birkfellner, F. Watzinger, F. Wanschitz, et al. Systematic Distortions in Magnetic Position Digitizers. *Med. Phys.*, 25(11):1142–1148, 1998.

[5] K. Dorfmüller. An Optical Tracking System for VR/AR-Applications. In A. H. M. Gervautz and D. Schmalstieg, editors, *Virtual Environments 99, Proceedings of the Eurographics Workshop*. Springer ComputerScience, Vienna, Austria, 1999.

[6] G. H. Golub and C. F. V. Loan. *Matrix Computations, 2nd ed.* Baltimore: Johns Hopkins University Press, 1989.

[7] M. C. Jacobs, M. A. Livingston, and A. State. Managing latency in complex augmented reality systems. In *Symposium on Interactive 3D Graphics*, pages 49–54, 185, 1997.

[8] K. Kanatani. *Geometric Computation for Machine Vision*. Oxford University Press, Oxford, 1993.

[9] V. Kindarenko. A Survey of Electromagnetic Position Tracker Calibration Techniques. In *Virtual Reality: Research, Development and Applications*, volume 5, pages 169–182, 2000.

[10] F. Madritsch and M. Gervautz. CCD-Camera Based Optical Beacon Tracking for Virtual and Augmented Reality. *Eurographics*, 3(15), 1996.

[11] O. Magneau, P.Bourdot, and R. Gherbi. 3D tracking based on infrared cameras. In *International Conference on Computer Vision and Graphics*, Zakopane, Poland, September 2002.

[12] D. W. Marquardt. An algorithm for least-squares estimation of nonlinear parameters. *Journal of the Society for Industrial and Applied Mathematics*, 11:431–441, 1963.

[13] J. Mulder, J. Jansen, and A. van Rhijn. An Affordable Optical Head Tracking System for Desktop VR/AR systems. In *Proceedings of 7th International Workshop on Immersive Projection Technology, 9th Eurographics Workshop on Virtual Environments*, Mai 2003.

[14] W. H. Press, S. A. Teukolsky, W. T. Vettering, and B. P. Flannery. *Numerical Recipes in C++:The Art of Scientific Computing, 2nd ed.* Cambridge: Cambridge University University Press, 2002.

[15] G. Reitmayr and D. Schmalstieg. An open software architecture for virtual reality interaction. In *ACM Symposium on Virtual Reality Software & Technology 2001*, 2001.

[16] M. Ribo, A. Prinz, and A. L. Fuhrmann. A new Optical Tracking System for Virtual and Augmented Reality. *IEEE Instrumentation and Measurement Technology Conference, Budapest, Hungary*, May 21-23 2001.

[17] M. Schnaider, B. Schwald, H. Seibert, and T. Weller. Medarpa - A Medical Augmented Reality System for Minimal-Invasive Interventions. In *Proceedings of the 11th Annual Medicine Meets Virtual Reality (MMVR) Conference*, Newport Beach, CA, USA, January 2003.

[18] B. Schwald, H. Seibert, and T. Weller. A Flexible Tracking Concept Applied to Medical Scenarios Using an AR Window. In *International Symposium on Mixed and Augmented Reality (ISMAR'02)*, Darmstadt, Germany, September 2002.

[19] E. Trucco, A. Fusiello, and V. Roberto. Robust motion and correspondences of noisy 3-d point sets with missing data. *Pattern Recognition Letters*, 20:889–898, 1999.

[20] S. Wesarg, T. H. Lauer, E. A. Firle, and C. Dold. Several marker segmentation techniques for use with a medical ar system - a comparison. In *Proceedings of the 17th CARS 2003, Elsevier*, page 1303, 2003.

[21] ARTtrack. http://www.ar-tracking.de, 2003.

[22] Medarpa. http://www.medarpa.de, 2003.

[23] Polaris. http://www.ndigital.com/polaris.html, 2003.